RECENT ADVANCES TO THE OPERATIONAL GOES WIND PROCESSING SYSTEM AT NESDIS

Jaime M. Daniels

NOAA/NESDIS
Office of Research and Applications
Washington D.C. 20233

Wayne Bresky

Raytheon STX Corporation
Lanham, Maryland 20706

Christopher Velden and Steven Wanzong

Cooperative Institute for Meteorological Satellite Studies (CIMSS)
Madison, Wisconsin 53706

ABSTRACT

Recent advances to regional and global numerical modeling requirements at NOAA's Environmental Modeling Center (EMC)/National Center for Environmental Prediction (NCEP) require higher quality satellite derived winds, particularly over the traditionally data void oceanic regions of the globe. In the past year, NOAA/NESDIS has responded by implementing an upgraded operational wind production suite in March 1998. This implementation provides high quality imager-based cloud-drift (IR) and water vapor motion winds at significantly increased spatial and temporal resolution. With increased computer resources, a ten-fold increase in the yield of "good" wind vectors for GOES-8 and GOES-10 are being generated every 3 hours for the Northern and Southern Hemisphere. Other advances included in this implementation include automated registration quality control, ensuring properly registered images used to produce the satellite wind vectors, and new quality control strategies employed for the satellite derived winds which encourages "buddy-checking" of different wind product types while retaining satellite-derived wind vectors in areas of high cyclonic or anticyclonic curvature. EMC/NCEP now uses these new operational NESDIS wind products in their global and regional data assimilation/numerical forecast systems. This paper and presentation will focus on highlighting the recent advances to the operational NESDIS wind product suite and the quality of these high spatial and temporal satellite wind vectors.

1. Introduction

Since the Third International Winds Workshop in June 1996, NOAA/NESDIS has been very active in improving its ability to generate high quality Atmospheric Motion Vectors (AMVs) from the GOES series of satellites. In March 1998, NOAA/NESDIS implemented an upgraded operational winds production suite. This implementation provided high quality imager-based cloud-drift IR and water vapor motion winds at significantly increased spatial and temporal resolution. New quality control (QC) strategies were implemented with this installation and additional or modified QC strategies have been more recently implemented. These QC strategies include: (1) Automated image registration; (2) Ensemble auto editing, where the various operational wind datasets are combined and intercompared for consistency; (3) Dual pass autoediting that relaxes rejection criteria for satellite winds around features of interest, like tropical storms, resulting in improved retention of satellite winds.

The NESDIS Office of Research and Applications (ORA) Forecast Products Development Team (FPDT) maintains an experimental winds production suite where experimental wind products are generated and validated and new algorithms are tested. Experimental winds currently being generated on a routine basis include low level visible winds and sounder-based water vapor winds derived from mid-level moisture sensitive bands. Other experiments being run routinely involve new targeting strategies aimed at improving the selection and location of wind tracers and increasing the number of low level wind tracers. The goals of this paper are to first provide an overview of the enhancements made to the NOAA/NESDIS winds processing system and highlight the new operational wind products, discuss the experimental wind data sets being generated on a routine basis by FPDT and the Cooperative Institute for Meteorological Satellite Studies (CIMSS), and to present results from the alternative targeting strategies recently developed.

2. Overview of the NOAA/NESDIS Wind Product System and the New Operational Wind Products

An overview of the operational NOAA/NESDIS winds processing system is shown in Figure 1. The major components of the system include: automated image registration quality control, target selection, wind target height assignment, target tracking, and automated quality control of derived winds.

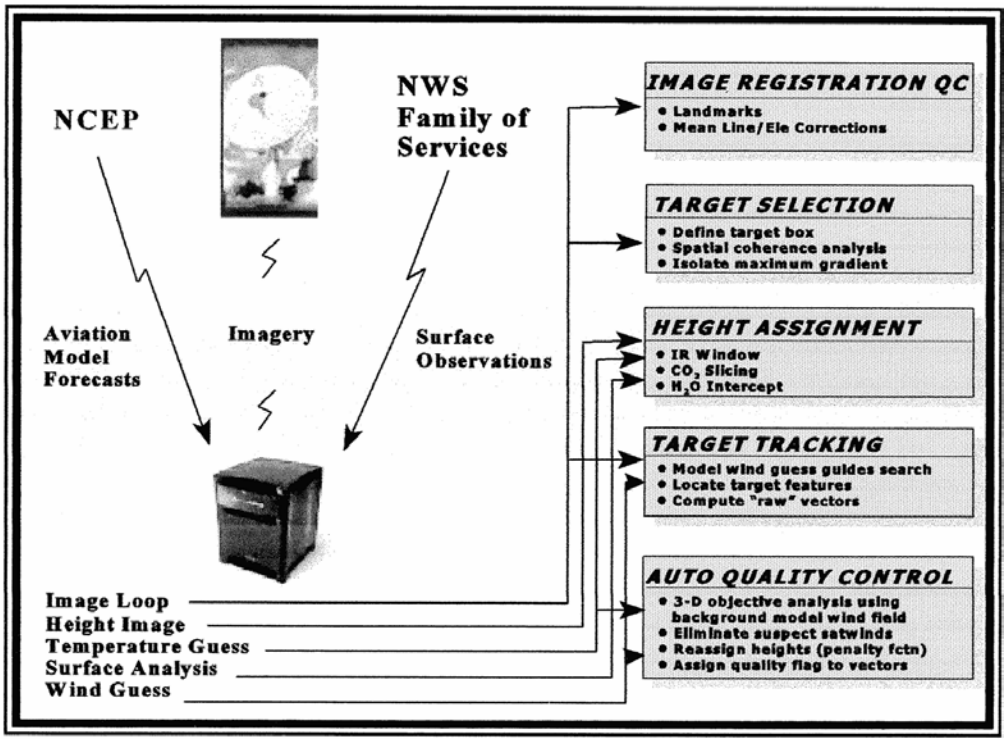

Figure 1 Overview of NOAA/NESDIS Winds Processing System

GOES imagery is acquired soon after ingest to build loops of imagery at 30 minute intervals. Aviation model forecast data is made available at 3 hour forecast intervals and at 1° x 1° resolution by the National Centers for Environmental Prediction(NCEP)/ Environmental Modeling Center(EMC). Surface observations are made available every hour by the National Weather Service (NWS). The first image in the loop is currently used for the target selection and height assignments. Subsequent imagery is used during the tracking phase. Finally, the EMC aviation model forecast data, used in the height assignment step is used in the final automated quality control (ie., autoeditor) step.

Operational cloud-drift (CD) and water vapor (WV) winds are produced for GOES-8 and GOES-10 at 3 hour intervals (00Z,03Z,06Z,09Z, 12Z, 15Z, 18Z, and 21Z). Approximately 6000 CD and 9000 WV winds are

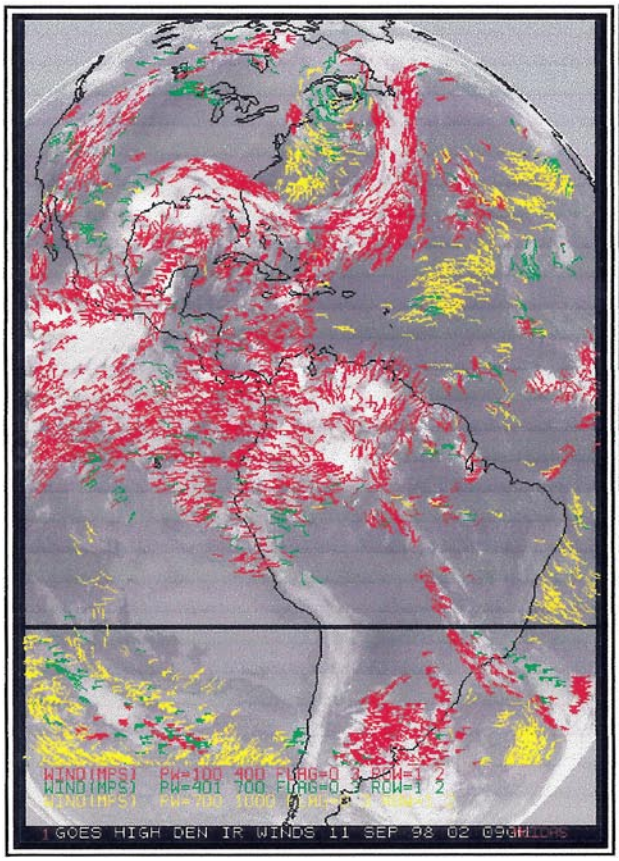

Figure 2a. Operational GOES-8 Cloud-drift Winds

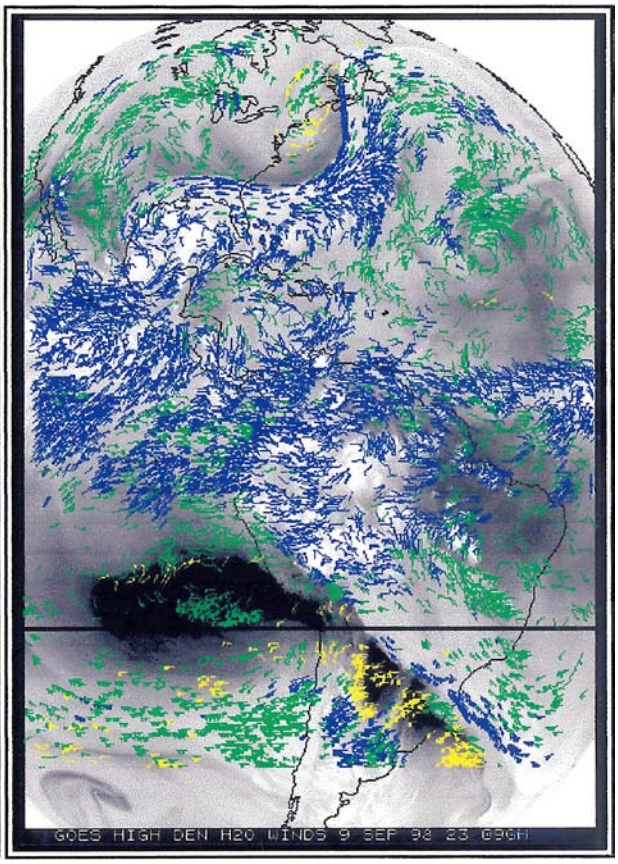

Figure 2b. Operational GOES-8 Water Vapor Winds

produced at each cycle for each spacecraft. Examples of these winds and the geographic coverage is shown in Figures 2a and 2b.

The operational satellite winds are currently being used operationally by the EMC in their regional and global models. The data are also being made available to the NWS regional weather offices and over the Global Telecommunication System (GTS) for the other major international modeling centers. Table 1 summarizes

the new operational wind datasets, their geographic coverage, frequency at which they are generated, and EMC's current use of their products in their various regional and global models.

EMC Assimilation Network Using Satwinds						
Product	***Coverage***	***Frequency***	***ETA/EDAS***	***NGM/RDAS***	***AVN/MRF/ GDAS***	***RUC-II***
Cloud-drift	NH,SH	8x/day	**YES** Ocean Land (South of 20S) +/- 1.5 hrs	**YES** Ocean Land (South of 20S) +/- 1.5 hrs	**YES** Ocean Land +/- 1.5hrs	**YES** Ocean Land (South of 20S) +/- 2.5 hrs
WV (cloud-top)	NH,SH	8x/day	**YES** Ocean Land (South of 20S) +/- 1.5 hrs	**YES** Ocean Land (South of 20S) +/- 1.5 hrs	**YES** Ocean Land +/- 1.5hrs	**YES** Ocean Land (South of 20S) +/- 2.5 hrs
WV (clear-air)	NH,SH	8x/day	**NO**	**NO**	**NO**	**YES**

Table 1 GOES satellite wind usage at the NOAA Environmental Modeling Center (EMC)

It is important to note that the quality of the CD and WV winds has not diminished as a result increasing the spatial density of these wind products. Figure 3 shows vector RMS and bias errors of the operational CD and WV winds relative to rawinsondes over the past year.

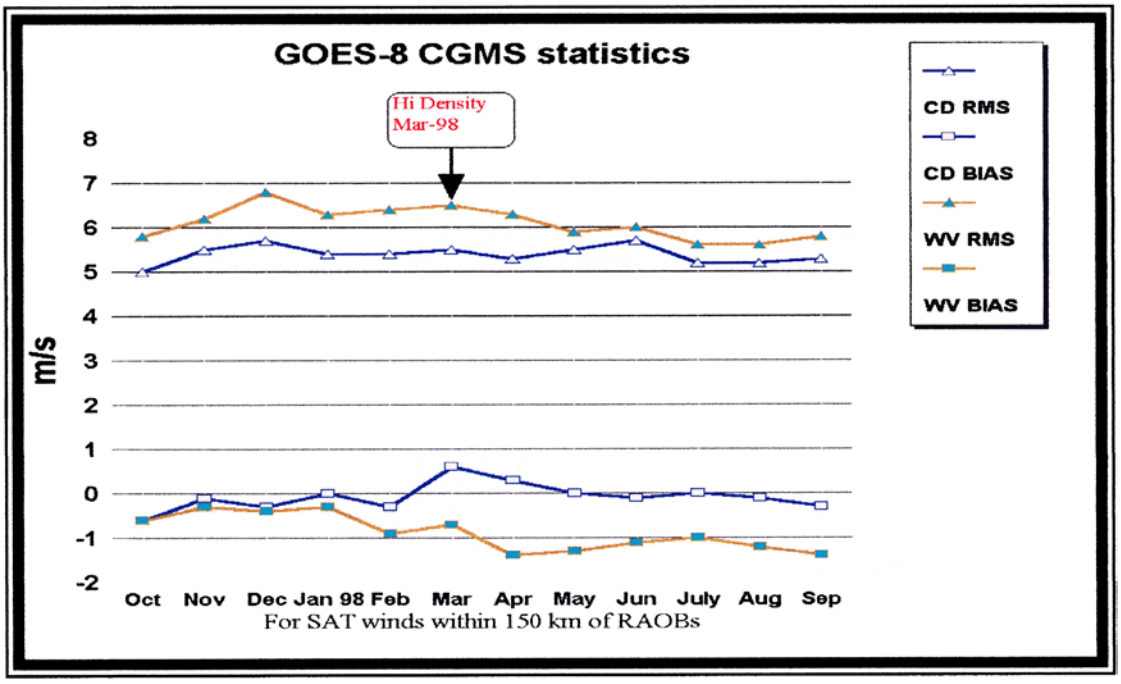

Figure 3 GOES-8 vector RMS Error and Speed Bias Error vs. Radiosonde

3. New Quality Control Measures Implemented

a) Automated Image Registration

Automated quality control of the image registration is a new and important addition to the NESDIS GOES winds processing suite. The quality of the satellite derived winds are much more sensitive to changes in registration than to errors in absolute navigation. Manual corrections to the winds imagery is no longer done. Automation of this function has become a necessity because of the increasing number of operational wind products generated and the increased frequency at which these products are generated. Figure 4 shows a schematic of the automated image registration quality control algorithm.

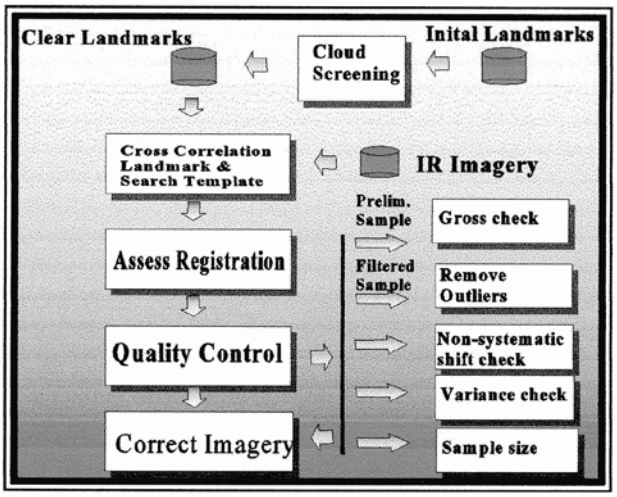

Figure 4 Automated Image Registration Quality Control Process

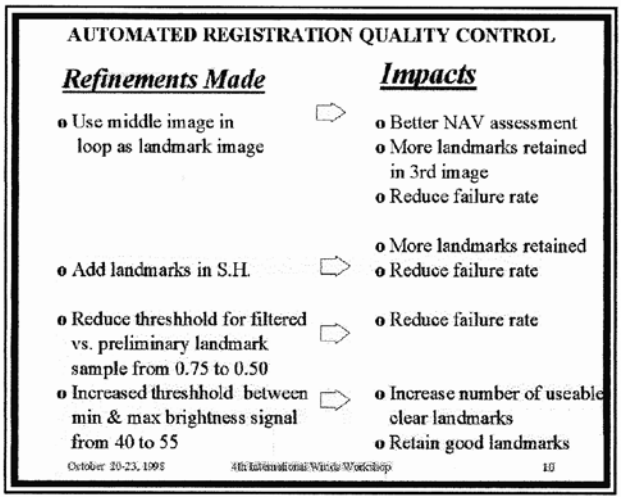

Figure 5 Refinements Made to Automated Image Registration Quality Control Algorithm

Nieman et al., 1996 discusses the initial image registration quality control algorithm installed in the NOAA/NESDIS winds processing system. This algorithm makes use of the pattern matching techniques used in the automated tracking algorithm (Merrill, 1989) to track land features of pre-determined landmarks deemed to be cloud free. Recent refinements have been made to the algorithm which have resulted in improved registration adjustments and fewer occurrences where the algorithm fails to arrive at a useable solution. These refinements are summarized in Figure 5.

The most significant refinement made to the algorithm involved the use of the middle image in the loop as the landmark image. In this scenario, the middle image is assumed to have perfect navigation. Adjustments are then made to the first and third images in order to line up their navigation to the middle image. The initial release of the algorithm used the first image in the loop as the landmark image. This posed problems for successfully retaining landmarks for the third image in the loop which was an hour later in time than the first image. Atmospheric effects (ie., clouds) and diurnal surface heating effects, particularly during sunrise and sunset, resulted in significantly fewer successful landmarks for the third image for all wind cycles. The significant number of landmark failures in the third image often led to a failure of the image registration algorithm to arrive at a useable solution. Using the middle image in the loop corrects this problem. A global landmark dataset is now used where additional landmarks have been added in the Southern Hemisphere. The addition of more landmarks in the Southern Hemisphere has increased the percentage of time the algorithm now successfully arrives at a mean line and element correction for Southern Hemisphere imagery. Another refinement made was to increase the difference threshold between the minimum and maximum brightness signal in the 15x15 box centered over the landmark. As a result, really good landmarks,

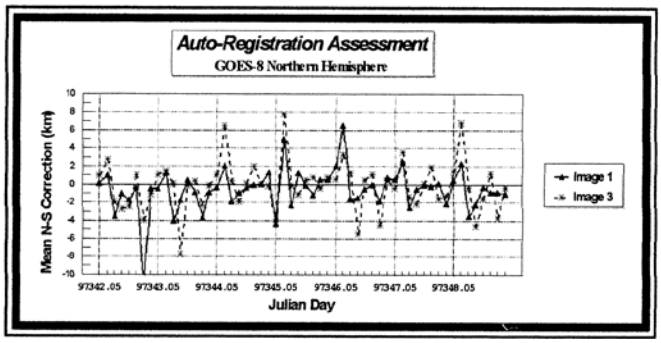

Figure 6a Mean N-S registration correction (km) for GOES-8 NH imagery

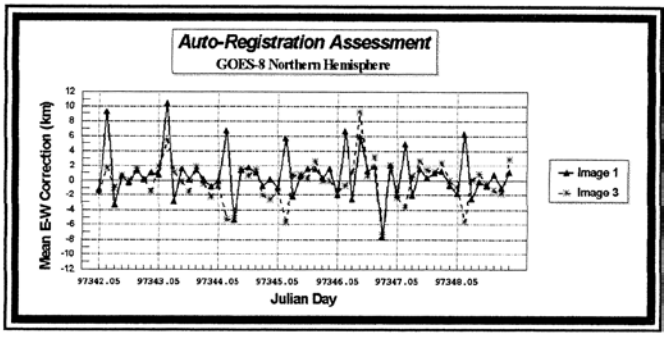

Figure 6b Mean E-W registration correction (km) for GOES-8 NH imagery

previously tossed, are now retained. All of these refinements have resulted in a more robust image registration algorithm which provides improved mean line and element adjustments. Figures 6a and 6b show the computed mean line and element corrections for the first and third images of GOES-8 Northern Hemisphere image loops for a week in December 1997. There are eight points per day corresponding to each wind cycle. For clarification purposes, a one line correction in Figure 6a corresponds to 4km, while one element correction in Figure 6b corresponds to 2.2km. For the most part, the computed mean line registration corrections are within plus or minus half line (+/- 2 km) which is well within image registration specifications of 2.25 km in the north-south direction. The same applies for the mean element corrections which are generally within plus or minus one element (+/- 2.2km), which is well within image registration specifications of 3.1 km in the east-west direction (Menzel and Purdom, 1994). What is evident is that the largest mean line and element corrections are generally determined for the 06Z wind cycles which correspond to the second data points of each day. The imagery used for the 06Z wind cycle are around local midnight where thermal heating of the satellite is at a maximum, contributing to a more difficult time with navigating the imagery. Figure 7 answers the question as to how often a line or element correction is suggested by the image registration quality control system. Overall, line or element corrections are suggested about 15% of the time over a 24 hour period. The 06Z and 09Z wind cycles contribute most significantly to this percentage because of the difficulties experienced with navigating imagery around satellite local midnight. If one excludes these cycles, then the percentage of time a line or element correction is suggested drops to around 5-10%.

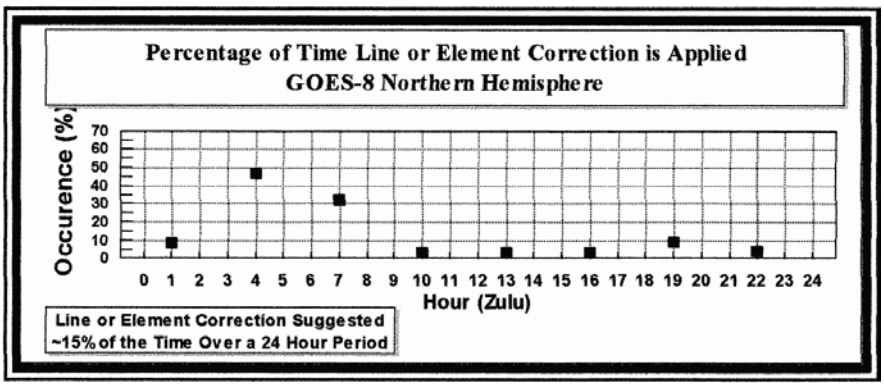

Figure 7 Percentage of time a mean line or element correction is applied for GOES-8 NH wind cycles

b) Ensemble and Dual Pass Autoediting

The current NESDIS winds processing suite now possesses the framework necessary for ensemble autoediting of all possible multispectral (visible, IR window, and three WV sensitive bands) wind datasets that can be generated from the GOES satellites. In the recently replaced operational winds system, each wind dataset was autoedited separately; there was no intercomparison of separate wind datasets during this process. At the present time, only the CD IR and WV winds are combined together during the autoeditor step of the process. When the visible and sounder based WV winds are added to the operational production suite, the three-dimensional coverage in the atmosphere depicted by the multi-spectral wind datasets will improve. This should strengthen the quality control process leading to improved satellite wind products which will have a better chance of surviving and impacting the data assimilation schemes of the major numerical weather prediction (NWP) centers.

A dual pass autoediting function is in place as a component of the final autoeditor step. As the name implies, the dual pass autoeditor process involves two executions of the autoeditor where one of the executions targets winds in a 15°x 15° box centered over a feature of interest. Rejection criteria, which involve tests using model forecast data, are relaxed over the area of interest in hopes of retaining a larger number of satellite winds around tight circulation features like tropical cyclones. The second execution of the autoeditor targets winds outside of the 15°xI5° box where the default (tighter) rejection criteria are used. Significantly more high level winds, for example, associated with the upper level outflow of a hurricane are retained. Figure 9b shows the high level winds in the cirrus outflow of Hurricane Georges. This information is important for a qualitative assessment of the wind flow in this region of the storm and as critical quantitative information for use in numerical analyses which often times do not adequately represent this flow.

4. Recent Experiments with Alternative Targeting Strategies

a) Targeting Low Level Wind Tracers Using IR Data

Inspection of GOES-10 imagery in the East Pacific Ocean often reveals a persistent and expansive stratocumulus deck which is not adequately sampled by the current operational NESDIS winds system. Figure 8a shows this problem where very few low level cloud drift winds are evident just off the west coast of California and to the north of the center of the large anticyclone. The reason for this is because all prospective IR targets undergo a spatial coherence analysis (Coakley and Bretherton, 1982) and are interrogated to ensure the maximum brightness gradient exceeds a threshold of 15 pixel brightness units. Experimental modifications have been made to the winds targeting routine in an effort to increase the number of low level

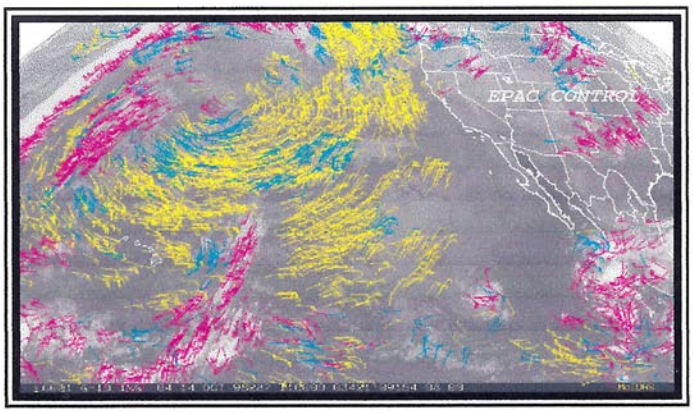

Figure 8a Control Case: GOES-10 cloud-drift IR winds

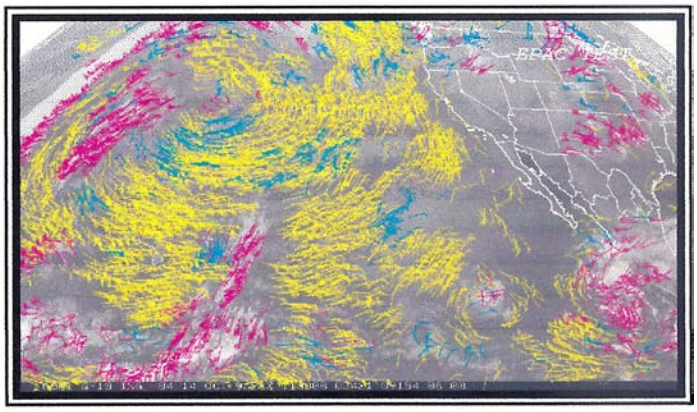

Figure 8b Test Case: GOES-10 cloud-drift IR winds

wind vectors in such situations. The modifications are applied only to targets below 550mb and include turning off the spatial coherence analyses and relaxing the minimum required brightness gradient threshold of 15 pixel brightness units to 4 pixel brightness units. The impact of these modifications on the number of low level winds has been dramatic. Figure 8b shows the test case where significant increases in the number of low level winds off the California coast and to the north of the center of the anticyclone are evident. Many more low level vectors are also generated in the low level flow around the expansive anticyclone.

Another example of this is shown in Figures 9a and 9b, which show the GOES-8 cloud-drift winds around Hurricane Georges for the control and test run, respectively. In the control run there are so few low level IR wind vectors that they provide little, if any, information on the low level wind field. The results of the test run, however, shows a substantial increase in the number of low level IR winds leading to a much better depiction of the low level wind field in the domain surrounding the storm. We have some concern, however, over a few wind vectors to the west south west of the storm which get through all of our quality control with incorrectly assigned heights. Clearly, these are cirrus tracers. Further inspection revealed that the water vapor intercept height assignment failed for these tracers, and as a result, the window height assignment was used which is a known to be problematic in such cases. We continue to look at this case more closely in hopes of arriving at a solution which allows for increased sampling of low level targets, but eliminates these problematic winds. Clearly, the inclusion of the visible winds will significantly contribute to characterizing the wind field at low levels, but only during periods of sufficient daylight.

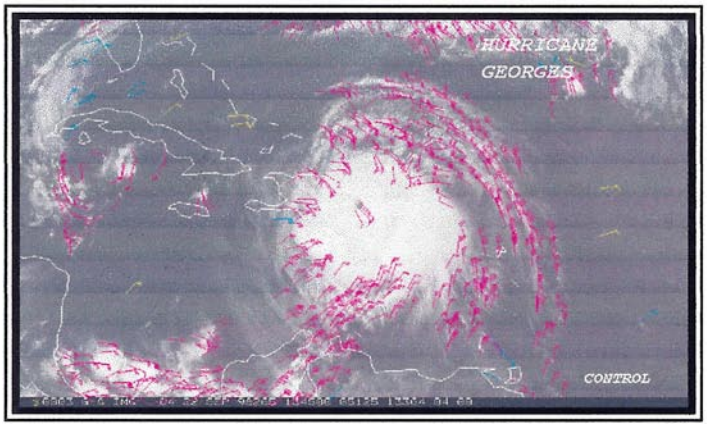

Figure 9a Control Case: Hurricane Georges

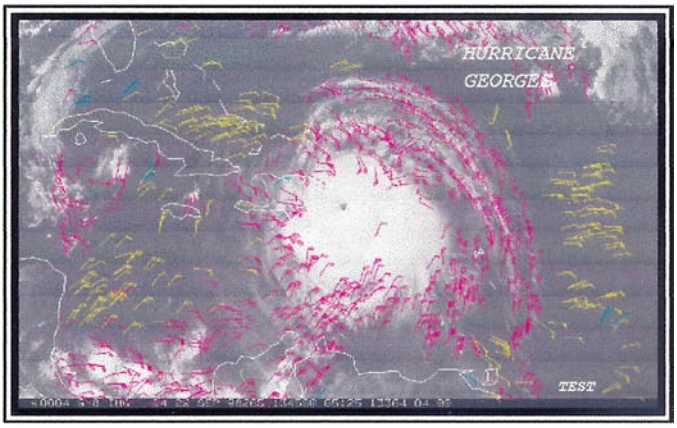

Figure 9b Test Case: Hurricane Georges

b) An Alternative Targeting Scheme

An alternative tracer selection algorithm has been developed which differs from the current operational one in how the gradient is computed for each pixel in the target box and in the position given to the tracer. Both algorithms then search for the maximum gradient, which exceeds some minimum brightness threshold, in identifying the tracer.

Schematics of the operational and experimental maximum gradient search algorithms are shown in Figures 10a and 10b. For the operational algorithm, the calculation of the gradient for each point in the target box involves multiple (up to 11) calculations of the absolute difference in brightness between the point in question (origin) and various endpoints. The gradient assigned to the origin point will be the maximum difference of these calculations and its location is determined by averaging the origin and end point line and elements. The tracer within the target box is assigned to that point having the largest gradient. The drawbacks of this approach include computation of the gradient over a variable distance and misplacement of the location of the maximum gradient. For the experimental algorithm, shown in Figure 9b, a centered finite difference calculation, where the pixel distance is taken into account, is performed for each point in the target

box. The advantage of this algorithm is that it provides for a more accurate representation of the two dimensional gradient at each point while assigning it to the correct line and element. The tracer is then assigned to that point in the target box containing the largest gradient.

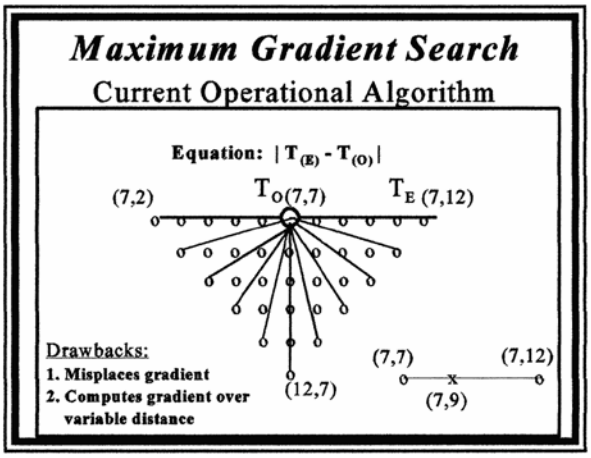

Figure 10a Current operational gradient search algorithm

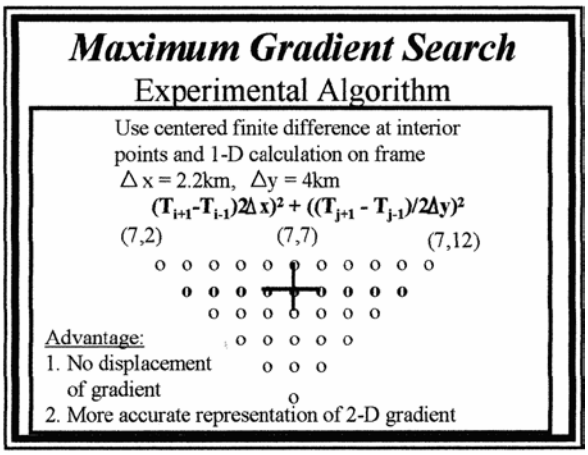

Figure 10b Experimental gradient search algorithm

The new algorithm has been run in parallel with the operational algorithm for a period of one month. The algorithm was tested on IR tracers. Results of this test indicate the new algorithm generates about the same number of tracers, but there is about a 10-15% increase in the number of winds produced which pass all of the internal quality control. This is a good result in itself. In an attempt to quantify the impact of this new algorithm on wind quality, we matched up the raw operational winds and the test raw winds against rawinsondes. Efforts were made to ensure that the operational and test winds were matched to the same rawinsondes, allowing for a more direct comparison of results between the two methods. Match statistics on the raw winds were done to eliminate the effects of the autoeditor quality control step which performs tracer height reassignments. In this way, we could more accurately measure impacts of wind quality due to the new tracer algorithm. These statistics are shown in Table 1.

WIND LEVEL	Avg. RMS		Speed Bias		Mean Raob Speed	Sample
	SAT	*GUESS*	*SAT*	*GUESS*		Size
HIGH						
Control	10.77	6.48	-2.56	-1.22	21.67	3200
Test	10.59	6.60	-2.18	-1.03	21.71	3193
MID						
Control	11.02	4.71	0.44	-1.17	13.02	1714
Test	10.91	4.67	0.41	-1.26	13.15	1736
LOW						
Control	10.24	3.63	0.62	-0.39	7.66	404
Test	10.16	3.86	-0.10	-0.58	7.88	451

Table 1 Raw cloud-drift wind statistics versus radiosonde. Control uses current operational gradient search algorithm. Test uses experimental gradient search algorithm.

As is evident from these statistics, significant improvements in the RMS error and bias are observed with the test cloud-drift IR winds at all levels. The improvements are even more significant when one considers the

colocated model guess statistics between the control run and the test run. Additional testing of the new algorithm is continuing which includes applying the new algorithm to water vapor imagery and assessing the impact of computing the gradient over 3 and 5 pixel distances.

5. Experimental Wind Products and Future Plans

Both ORA/FPDT and CIMSS are routinely generating and validating experimental visible wind and sounder (7.0µm and 7.3µm) water vapor wind products. ORA/FPDT is currently generating a 2km visible wind datasets using 30 minute interval imagery every 3 hours during daylight hours for GOES-8 and GOES-10. An example of this 2km visible wind is shown in Figure 11. CIMSS is routinely generating a 4km visible wind product using 30 minute interval imagery and a special lkm visible wind product using 15 minute interval imagery in tropical storm environments. Veldon et.al, 1998 discusses these new wind products and their applications. The visible wind products are currently being made available to the EMC for regional and global model impact studies. The addition of the visible wind products to the operational suite of NESDIS wind products will likely occur in late spring of 1999 after EMC model impact assessments are completed and NESDIS operations completes its year 2000 compliance testing of all of its systems.

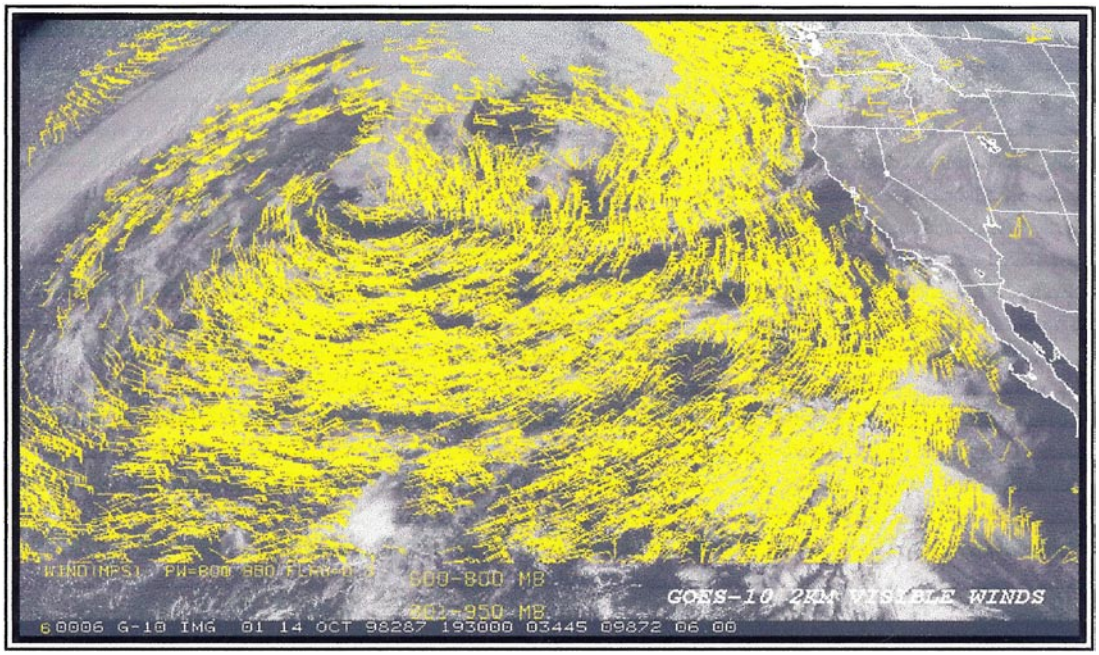

Figure 11 Experimental GOES-10 2km Visible Wind Product Current

NESDIS plans also call for the generation of even higher temporal resolution winds on an experimental basis. The current winds processing system has been designed with this capability in mind. Wind datasets can be generated on an hourly basis. The Rapid Update Cycle (RUC) at EMC will be the targeted recipient of these winds and model impact studies using these high temporal frequency datasets are planned over the next year.

6. References

Coakley, J. and F. Bretherton, 1982: Cloud cover from high resolution scanner data: detecting and allowing for partially filled fields of view. *J. Geophys. Res.*, **87**(C7) 4917-4932.

Menzel, W.P. and J.F.W. Purdon, 1994: Introducing GOES-I: The first of a new generation of geostationary operational environmental satellites. *Bull. Amer. Meteor. Soc.*, **75**, 757-781.

Merril, R., 1989: Advances in the automated production of wind estimates from geostationary satellite imaging. *Proc. Fourth Conf Satellite Meteorology,* San Diego, CA., Arner. Meteor. Soc., 246-249.

Nieman, S, J. Daniels, D. Gray, S. Wanzong, C. Velden, W. Menzel, 1996: Recent performance and upgrades to the GOES8/9 Operational Cloud-Motion Vectors, Third Intl.Winds Workshop, Monte-Verita-Ascona, Switzerland, 31-36.

Velden, C., C. Hayden, S. Nieman, W.Menzel, S. Wanzong, and J. Goerss, 1997: Upper-Tropospheric Winds Derived from Geostationary Satellite Water Vapor Observations. *Bull. Amer. Meteor. Soc.*, **78**,173-195.

Velden, C., S. Wanzong, and W. Menzel, 1998: An update on CIMSS winds development. *Fourth Intl. Winds Workshop.*